INFLUENCE OF LITHIUM HYDROXIDE ON ALKALI-SILICA REACTION

David Bulteel[1,*], Eric Garcia-Diaz[1], Patrick Dégrugilliers[1]

[1]Ecole Nationale Supérieure des techniques industrielles et des Mines de Douai, Département génie civil et environnemental, 941 rue Charles Bourseul, B.P. 10838, 59508 DOUAI, France

Abstract

Several papers show that the use of lithium limits the development of Alkali-Silica Reaction (ASR) in concrete. The aim of our study is to improve the understanding of lithium's role on the alteration mechanism of ASR.

Our approach uses a chemical method which allows a quantitative measurement of the specific degree of reaction of ASR. We use a chemical concrete sub-system called model reactor composed of the main ASR reagents: reactive aggregate, portlandite and alkaline solution. Different reaction degrees are measured and compared for different alkaline solutions: NaOH, KOH and LiOH.

Alteration by ASR is observed with the same reaction degrees in the presence of NaOH and KOH, accompanied by the consumption of hydroxyl concentration. On the other hand with LiOH, ASR is very limited. Reaction degree values evolve little and the hydroxyl concentration remains about stable.

These observations demonstrate that lithium ions have an inhibitor role on ASR.

Keywords: alkali-silica reaction, reactive aggregate, reaction degree, inhibitor, lithium

1 INTRODUCTION

It is well known that alkali-silica reaction (ASR) poses a durability problem to concrete. It can induce cracking and damage in concrete structures. The origin of the reaction is a chemical reaction between four essential compounds included in concrete: moisture, a sufficiently high concentration of hydroxyl, a pessimum amount of reactive silica in the aggregate and the presence of portlandite. Different methods have been made to mitigate or prevent ASR. The addition of lithium salts is one of these methods. The first reported use of lithium salts to control ASR was in 1951 [1]. Since, many papers on mortar bars or concrete [2-10] have reported reducing or suppressive effects on expansion due to ASR. But the mechanism or mechanisms by which lithium acts, are not well understood [11]. Like Mitchell et al. [12], we work on a chemical concrete sub-system. Our model reactors consist of reactive aggregate, portlandite and alkaline solution: NaOH, KOH or LiOH. The aim of our study is to improve the understanding of lithium's role on alteration mechanism of ASR by quantitative measurements of specific reaction degrees and alkaline species.

2 MATERIALS AND METHODS

2.1 Reactive aggregate used

The material used in this study is a "chert type" reactive aggregate coming from the north of France. The choice of this material is due to its reactivity so as to achieve the comparison of NaOH, KOH and LiOH action on ASR which is the aim of our study. A characterisation has been given by Bulteel et al. [13]. A short description follows. X-ray fluorescence analysis gives a composition close to 99% SiO_2 (Table 1 with CO_2 value determined by thermogravimetric analysis). X-ray diffraction analysis detects only quartz lines in this aggregate. Elements other than Si have not been studied. The quartz crystal lattice is characterised by ^{29}Si solid NMR spectroscopy [14]. This crystal lattice is constituted by Q_4 SiO_2 tetrahedra and Q_3 $SiO_{5/2}H$ "silanol" tetrahedra. The Q_3 molar fraction measured by thermogravimetry is close to 0.07.

The mineralogy of the material is determined by optical microscopy. This aggregate is essentially micro to crypto crystalline (microquartz) and contains radial fibers (chalcedony). The crystal size is variable but in general particularly small: a few microns. However, a few grains present a development of chalcedony zones. Carbonate fragments (calcite) are present and this is in agreement

* Correspondence to: bulteel@ensm-douai.fr

with the low content in calcium measured by XRF (Table 1). Red spots indicate the presence of the iron oxide traces detected by XRF (Table 1).

The material has a specific area of 0.97 m^2/g by BET analysis and a specific porosity of 3 mm^3/g by BJH analysis. As the external surface calculated from size distribution data is as low as 0.008 m^2/g, we can conclude that the reactive sites of the studied aggregate are mainly located in a kind of "internal surface". Its absolute density measured by helium pycnometer analysis is about 2.595g/cm^3.

This aggregate is crushed to 0.16-0.63 mm and homogenized for this study.

2.2 Determination of reaction degrees

The determination of reaction degrees is based on ASR mechanism which is described using different models [15-19] and can be written in two main steps (eg. here for KOH):
Formation of Q_3 sites (step 1) due to a first siloxane bonds breaking up by hydroxyl attack:

$$SiO_2 + KOH \rightarrow SiO_{5/2}K + 0.5\ H_2O \quad (1)$$

From a structural point of view, SiO_2 represents a Q_4 silicon tetrahedron sharing 4 oxygens with 4 neighbours, and using a simplified notation, $SiO_{5/2}K$ represents the Q_3 tetrahedron sharing 3 oxygens with 3 neighbours.
Dissolution of silica (step 2) due to continued hydroxyl attack of the Q_3 sites to form Q_0 silica ions:

$$SiO_{5/2}K + KOH + 0.5\ H_2O \rightarrow (H_2SiO_4)^{2-} + 2\ K^+ \quad (2)$$

These silica ions respect the Iler equilibrium [20] according to pH.
Afterwards, precipitation of silica ions by the cations of the pore solution of concrete is liable to C-S-H and/or C-K-S-H phase formation.

In this study, the use of the chemical method [14] allows us to quantify specific reaction degrees of ASR based on steps (1) and (2), which are defined as follows:

$$FMQ_4 = \text{moles of } Q_4 \text{ sites/moles of initial silica} \quad (3)$$

$$FMQ_3 = \text{moles of } Q_3 \text{ sites/moles of initial silica} \quad (4)$$

$$FMQ_0 = \text{moles of dissolved sites/moles of initial silica} \quad (5)$$

$$FMQ_4 + FMQ_3 + FMQ_0 = 1 \quad (6)$$

Formed Q_0 silica ions can remain in solution or can be precipitated:

$$FMQ_0 = FMQ_{0solution} + FMQ_{0precipitated} \quad (7)$$

$$FMQ_{0solution} = \text{moles of silica ions in solution/moles of initial silica} \quad (8)$$

$$FMQ_{0precipitated} = \text{moles of precipitated silica/moles of initial silica} \quad (9)$$

2.3 Assessment of reaction progress

General

The chemical method based on using a model reactor allows the determination of reaction degrees, obtained by solid and liquid characterisation at different reaction times, and uses the following protocol organised in different procedures [21]:

Start:

A mix of 1g of 0.16-0.63 mm crushed aggregate and 0.5g $Ca(OH)_2$ is introduced in a closed stainless steel container. After 30 minutes preheating up to 80°C, 10 ml of 0.79 mol/l KOH is added. The container is then autoclaved at different times at 80°C to accelerate ASR under controlled temperature.

Procedure 1:

After the reaction, the aggregate is constituted by Q_4 tetrahedra that have not reacted (sound silica) and by the Q_3 tetrahedra (i.e. $SiO_{5/2}K$, $SiO_{5/2}CaSiO_{5/2}$ and $SiO_{5/2}H$) which constitute the degraded silica. In this procedure, a large part of the alkaline solution is extracted and filtered to 0.45 µm. Solution's silica concentration ($FMQ_{0solution}$ defined in Equation 8) is determined by ICP-OES analyses after HNO_3 acidification with Varian 720-ES instrument. Alkaline concentration is assessed by titration analyses. From these two parameters, hydroxyl concentration is determined [22].

Of two different reaction vessels', the first is treated by procedure 2a, the second is treated by procedure 2b.

Procedure 2a (acid alternative):

Selective acid digestion with 250 ml cold 0.5M HCl solution followed by filtration leads to the removal of the soluble reaction products ($(H_2SiO_4)^{2-}$, $(H_3SiO_4)^-$, K^+ , Ca^{2+}, C-S-H and/or C-K-S-H) but also reagents (KOH and $Ca(OH)_2$). During this chemical treatment the Q_3 tetrahedra $SiO_{5/2}K$ and/or $SiO_{5/2}CaSiO_{5/2}$ are protonated to form silanols $SiO_{5/2}H$ with a release of K^+ and/or Ca^{2+} cations.

The efficiency of the acid rinse is quickly controlled by X-ray fluorescence: the SiO_2 content of the remaining solid must be about 99%. In this case, measurements of the remaining solid characterised by ^{29}Si solid NMR spectroscopy show residual SiO_2 Q_4 tetrahedra and $SiO_{5/2}H$ Q_3 tetrahedra and confirme the absence of silica gel precipitation after the acid treatment [14].

After thermal treatment of the residual solid at 1000°C, the silanol groups are condensed to give back silica Q_4 and release water following :

$$2SiO_{5/2}H \xrightarrow{1000°C} 2SiO_2 + H_2O \quad (10)$$

Measurement of the water loss by thermogravimetry allows calculation of the quantity of Q_3 tetrahedra in the aggregate sample (FMQ_3 defined in Equation 4). The weight of the residual silica makes it possible to determine by difference the quantity of dissolved silica (FMQ_0 defined in Equation 5). With silica concentration in the solution measured according to procedure 1 ($FMQ_{0solution}$), precipitated silica ($FMQ_{0precipitated}$) is determined by Equation 7.

Procedure 2b (alkaline alternative):

Filtration with ethyl alcohol allows us to preserve solid and mainly $Ca(OH)_2$. Measurement of the mass loss by thermogravimetry (about 450°C for the dehydration of portlandite especially and sometimes about 700°C for the CO_2 loss in case of carbonate portlandite for the experiment) allows calculation of the quantity of residual portlandite and so the content of consumed portlandite.

The experimental procedure above for KOH is duplicated using either NaOH or LiOH solution. Results from all three runs are reported below.

3 RESULTS

3.1 Reaction progress with time

The variation of molar fractions FMQ_4, FMQ_3 and FMQ_0 with time as shown in Figures 1, 2 and 3 demonstrates the very different effects of LiOH compared to NaOH and KOH. Globally, the molar fractions evolution is similar for KOH and NaOH. Q_4 tetrahedra are highly consumed by hydroxyl attack. Moreover in KOH case, the assumption based on a representation of the aggregate only with Q_3 and Q_4 tetrahedra find its limit with the "negative value" for FMQ_4 in Figure 1. Indeed, at a very high alteration, the presence of Q_2 sites is no longer negligible, hence a bad value of FMQ_4. FMQ_0 increases up to 72 and 120 hours respectively for NaOH and KOH to reach an asymptotic value of about 0.5. The content of Q_3 sites increases after a short plateau of about 24 hours which corresponds to the initial Q_3 sites value ($FMQ_3 \approx 0.07$). On the other hand, the molar fractions evolution from LiOH is totally different. FMQ_4 passes from 0.93 to about 0.8 indicating only a small consumption by hydroxyl attack. In addition, formed Q_3 and Q_0 quantities are very small with FMQ_3 from 0.07 to about 0.15 and FMQ_0 close to 0.06 in spite of a longer time of attack (336 hours).

Figures 4, 5 and 6 show FMQ_0 dissolved silica evolution which corresponds to $FMQ_{0solution}$ free silica ions in solution and $FMQ_{0precipitated}$ precipitated silica (Equation 7) according to time. With

KOH and NaOH, FMQ_0 increases up to 0.5. Between 0 and 14 hours, dissolved silica precipitates but after 14 hours, free silica ions appear and increase while the precipitation continues in KOH case and remains stable in NaOH case. With LiOH, the result is completely different. FMQ_0 is not higher than 0.06 and all dissolved silica ions precipitate.

Q_3 sites content according to dissolved silica is shown in Figure 7. For KOH and NaOH, the curves are globally similar. In the first part, dissolved silica formation is favoured with FMQ_0 increasing from 0 to close to 0.3 while FMQ_3 has gone up from 0.07 to 0.1 only. In the second part, Q_3 sites content is multiplied by 5 to 7 in comparison with initial value. Inversely, with LiOH, the cloud of point close to the origin shows a very small content of FMQ_0 and FMQ_3 is only multiplied by 2.

3.2 Evolutions of alkaline species

Figures 8, 9 and 10 show evolutions of 3 alkaline species: alkaline concentration, hydroxyl concentration and consumption of portlandite content according to molar fraction of dissolved silica (FMQ_0). As different reaction degrees, alkaline species evolution is visible enough with KOH and NaOH compared to LiOH. Figure 8 with KOH, after a short plateau, $FMQ_0 = 0.06$, hydroxyl concentration falls throughout the reaction. Up to $FMQ_0 = 0.2$, alkaline concentration is relatively stable then decreases from 0.76 to 0.54. Consumption of portlandite content increases for the reaction to reach more than 0.8. Figure 9 with NaOH, alkaline concentration evolves between 0.79 and 0.7. Hydroxyl concentration falls very quickly to reach about 10^{-4} mol/l. Consumption of portlandite content continuously increases to reach close to 0.9. In LiOH case (Figure 10), evolution of alkaline species is totally different since it makes almost no progress; besides FMQ_0 does not exceed 0.06 instead of 0.6 for the two other cases. Alkaline concentration and hydroxyl concentration are identical and remain at high values: 0.75 mol/l. Portlandite content is little consumed (less than 0.1).

4 DISCUSSION

Through all the results, two totally different behaviours are observed. On the one hand, model reactors with KOH and NaOH present a similar evolution and will be discussed together and on the other hand, model reactor with LiOH is very different and will be compared to the two others.

In KOH and NaOH cases (Figures 1 and 2), Q_4 molar fraction falls while Q_3 and Q_0 molar fractions increase: ASR progresses. Indeed, from Equations 1 and 2, the Q_4 sites give Q_3 sites and Q_0 dissolved silica. This high proportion of final dissolved silica shows that Equation 2 plays an important part in this experiment where initial hydroxyl concentration is high with 0.79 mol/l. The high content of Q_3 sites is characteristic of a silica gel formed by the hydroxylic break-up of the siloxane bonds, probably following a topochemical mechanism. The big increase of FMQ_3 shows that the creation of Q_3 sites prevails over the dissolution reaction in spite of high FMQ_0 (Figure 7). Equation 1 is more important than Equation 2. From Equations 1 and 2, the development of ASR also consumes hydroxyl ions (Figures 8 and 9) involving a reduction in hydroxyl concentration and portlandite consumption. Indeed, portlandite dissolves to supply hydroxyl ions available for the reaction and also releases calcium ions. Then, these calcium ions take part in the precipitation of dissolved silica in the form of C-S-H which also could fix alkalis (Figures 4 and 5). In these cases, the reaction is so developed that all dissolved silica does not precipitate and remain in solution. Alkaline concentration remains relatively high because the consumption of (OH^-) hydroxyl ions is balanced by the appearance of silica ions in solution ($(H_2SiO_4)^{2-}$ and/or $(H_3SiO_4)^-$).

In LiOH case, reaction degrees (specific of ASR) and alkaline species are completely different. They evolve slightly compared to KOH and NaOH. Indeed, FMQ_4, FMQ_3 and FMQ_0 change only a little (Figure 3) indicating a very small hydroxyl attack according to Equation 1 and 2 despite a high concentration with 0.79 mol/l. Thus, few Q_3 sites and Q_0 dissolved silica are formed (Figure 7). Hydroxyl concentration remains high through lack of the hydroxylic break-up of the siloxane bonds (Figure 10). Portlandite which plays the role of hydroxyl reserve is scarcely consumed. A very small quantity of dissolved silica is totally and immediately precipitated with calcium ions (Figure 6). The absence of silica concentration in solution gives an alkaline concentration equal to the hydroxyl concentration.

These results show that ASR progresses very little with the presence of LiOH even for a very long time in very severe conditions in the model reactor. In these conditions, LiOH is an inhibitor of ASR and not only a delaying agent.

In previous works [23], we proposed ASR mechanism where expansion was in relation with increase of FMQ_3. In this study, LiOH induces a few new Q_3 sites hence low expansion risk. But the problem is how can we explain the very small quantity of formed products with such a high hydroxyl

concentration with 0.79 mol/l whereas with NaOH and KOH, it is extensively sufficient to develop ASR? After Feng et al. [11] which resumed different mechanisms, a small quantity of formed products would have no expansive nature and would perhaps form a "barrier" to stop hydroxyl attack.

5 CONCLUSIONS

Use of model reactors constituted from reactive aggregate, portlandite and alkaline solution like NaOH, KOH or LiOH and at 80°C allows us to have the must favourable conditions to develop ASR. Our study measures specific and quantitative ASR reaction degrees and also alkaline species. The results led to the following conclusions:

(1) With NaOH and KOH, reaction degrees and alkaline species evolve a lot hence ASR developes. On the other hand, with LiOH, the result is totally different as reaction degrees and alkaline species show small evolutions. ASR progresses very little. LiOH is an inhibitor of ASR and not only a delaying agent.

(2) In literature, the absence of expansion on mortar bars or concretes with LiOH could be explained thanks to low formation of Q_3 sites in the aggregate. Indeed, in previous works [23], we proposed the ASR mechanism where expansion was in relation with the increase of Q_3 sites. LiOH induces a few new Q_3 sites hence low expansion risk.

(3) LiOH inhibits ASR because the quantity of formed ASR products is very small but why are there so few ASR products with such a high hydroxyl concentration (0.79 mol/l) whereas with NaOH and KOH, it is extensively sufficient to develop ASR? A small quantity of formed products would have no expansive nature and would perhaps form a "barrier" to stop hydroxyl attack. Future investigations will try to develop the identification of formed products for a better comprehension of the mechanism(s).

6 REFERENCES

[1] McCoy, WJ, and Cauldwell, AG (1951): New approach to inhibiting alkali aggregate expansion. Journal of America Concrete Institute (22): 693-706.

[2] Stark, DC (1992): Lithium salt admixtures – An alternative method to prevent expansive alkali-silica reactivity. Proceedings of the 9th International Conference on Alkali-Aggregate Reaction, London, UK: 1017-1025.

[3] Lumley, JS (1997): ASR suppression by lithium compounds. Cement and Concrete Research (27): 235-244.

[4] Ramachandran, VS (1998): Alkali-aggregate expansion inhibiting admixtures. Cement and Concrete Composite (20): 149-161.

[5] Diamond, S, and Ong, S (1992): The mechanisms of lithium effects on ASR. Proceedings of the 9th International Conference on Alkali-Aggregate Reaction, London, UK: 269-278.

[6] Thomas, MDA, Hooper, R, and Stokes, D (2000): Use of lithium-containing compounds to control expansion in concrete due to alkali-silica reaction. Proceedings of the 11th International Conference on Alkali-Aggregate Reaction, Quebec, Canada: 783-792.

[7] Kawamura, M, and Kodera, T (2005): Effects of externally supplied lithium on the suppression of ASR expansion in mortars. Cement and Concrete Research (35): 494-498.

[8] Mo, X (2005): Laboratory study of LiOH in inhibiting alkali-silica reaction at 20°C: a contribution. Cement and Concrete Research (35): 499-504.

[9] Mo, X, Jin, T, Li, G, Wang, K, Xu, Z, and Tang, M (2005): Alkali-aggregate reaction suppressed by chemical admixture at 80°C. Construction and Building Materials (19): 473-479.

[10] Collins, CL, Ideker, JH, Willis, GS, and Kurtis, KE (2004): Examination of the effects of LiOH, LiCl, and $LiNO_3$ on alkali-silica reaction. Cement and Concrete Research (34): 1403-1415.

[11] Feng, X, Thomas, MDA, Bremner, TW, Balcom, BJ, and Folliard, KJ (2005): Studies on lithium salts to mitigate ASR-induced expansion in new concrete: a critical review. Cement and Concrete Research (35): 1789-1796.

[12] Mitchell, LD, Beaudoin JJ, and Grattan-Bellew P (2004): The effects of lithium hydroxide solution on alkali silica reaction gels created with opal. Cement and Concrete Research (34): 641-649.

[13] Bulteel, D, Rafai, N, Degrugilliers, P, and Garcia-Diaz, E (2004): Petrography study on altered aggregate by alkali-silica reaction. Materials Characterization (53): 141-154.

[14] Bulteel, D, Garcia-Diaz, E, Vernet, C, and Zanni, H (2002): Alkali-silica reaction: a method to quantify the reaction degree. Cement and Concrete Research (32): 1199-1206.
[15] Dent Glasser, LS, and Kataoka, N (1981): The chemistry of alkali-aggregate reaction. Cement and Concrete Research (11): 1-9.
[16] Poole, AB (1992): Alkali silica reactivity mechanisms of gel formation and expansion. Concrete Society Publications CS. Proceedings of the 9th International Conference on Alkali-Aggregate Reaction, London, UK: 782-789.
[17] Urban, S (1987): Alkali silica and pozzolanic reactions in concrete. Part 1: Interpretation of published results and a hypothesis concerning the mechanism. Cement and Concrete Research (17): 141-152.
[18] Wang, H, and Gillott, JE (1991): Mechanism of alkali-silica reaction and significance of calcium hydroxide. Cement and Concrete Research (21): 647-654.
[19] Dron, R (1990): Thermodynamique de la reaction alkali-silice. Bulletin de liaison des Laboratoires des Ponts et Chaussées (166): 55-59.
[20] Iler, RK (1979): The chemistry of silica. Wiley-Interscience Publication. New York, USA: 835.
[21] Bulteel, D, Riche, J, Garcia-Diaz, E, Rafai, N, and Degrugillers, P (2004): Better understanding of ASR mechanism thanks to petrography study on altered flint aggregate. Proceedings of the 12th International Conference on Alkali-Aggregate Reaction, Beijing, China: 69-78.
[22] Bulteel, D (2000): Quantification de la réaction alkali-silice: application à un silex du Nord de la France. PhD thesis, Université des sciences et technologies de Lille, France : pp301.
[23] Garcia-Diaz, E, Riche, J, Bulteel, D, and Vernet, C (2006): Mechanism of damage for the alkali-silica reaction. Cement and Concrete Research (36): 395-400.

TABLE 1: Whole rock main element composition of the reactive aggregate in wt% of oxides obtained by X-ray fluorescence analysis (XRF). Species not listed are near or under LLD.

main elements	wt %
SiO_2	98.9
Fe_2O_3	0.4
CaO	0.3
$*CO_2$	0.2
Al_2O_3	0.2
Sum	100.0
*: CO_2 was measured gravimetrically as ignition loss LOI	

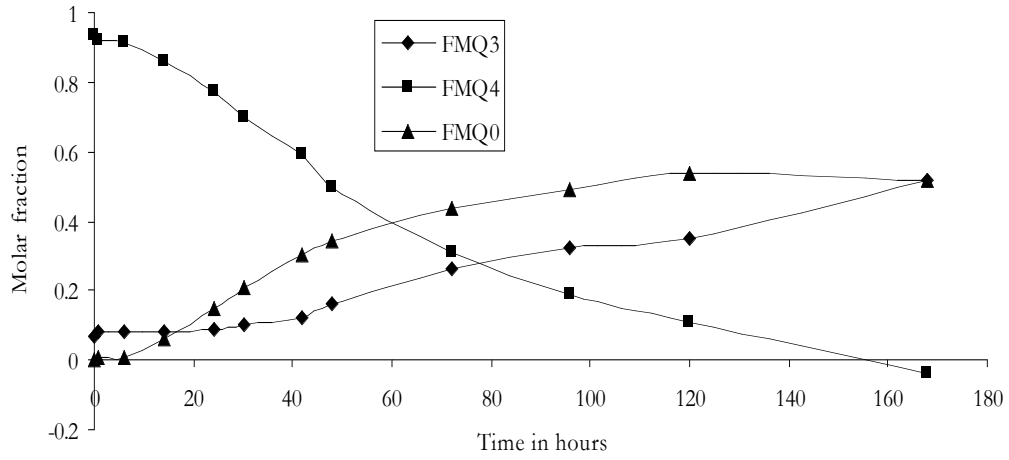

Figure 1: Molar fractions of Q_4, Q_3 and Q_0 according to time for the model reactor with KOH.

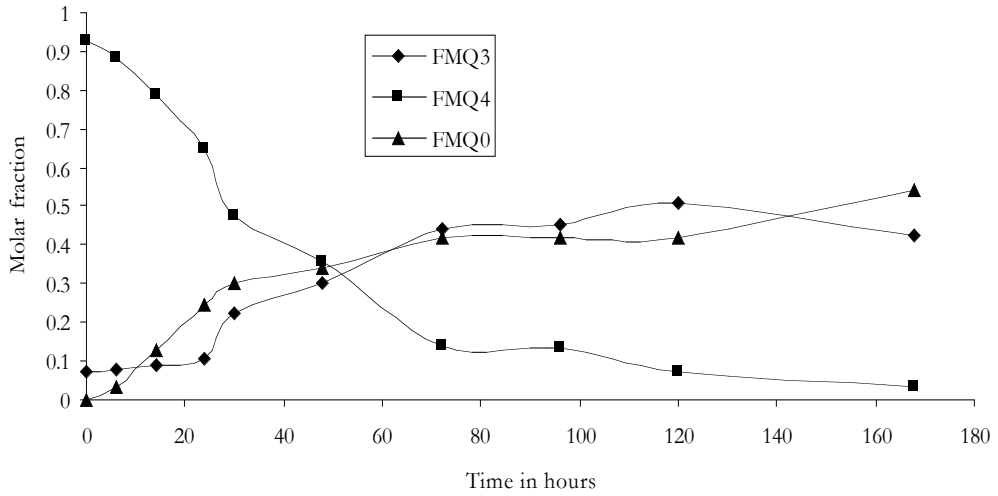

Figure 2: Molar fractions of Q_4, Q_3 and Q_0 according to time for the model reactor with NaOH.

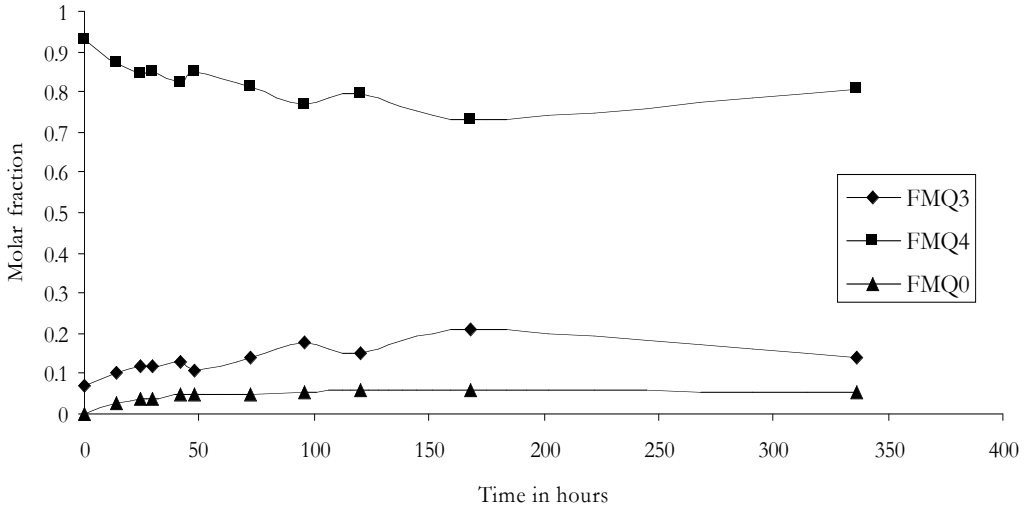

Figure 3: Molar fractions of Q_4, Q_3 and Q_0 according to time for the model reactor with LiOH.

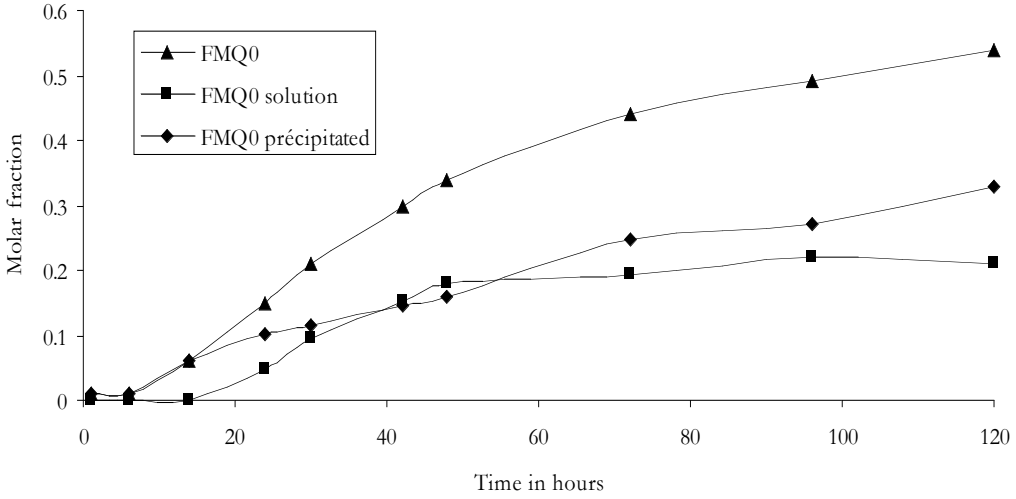

Figure 4: Molar fraction of Q_0 constituted to molar fractions of $Q_{0solution}$ and $Q_{0precipitated}$ according to time for the model reactor with KOH.

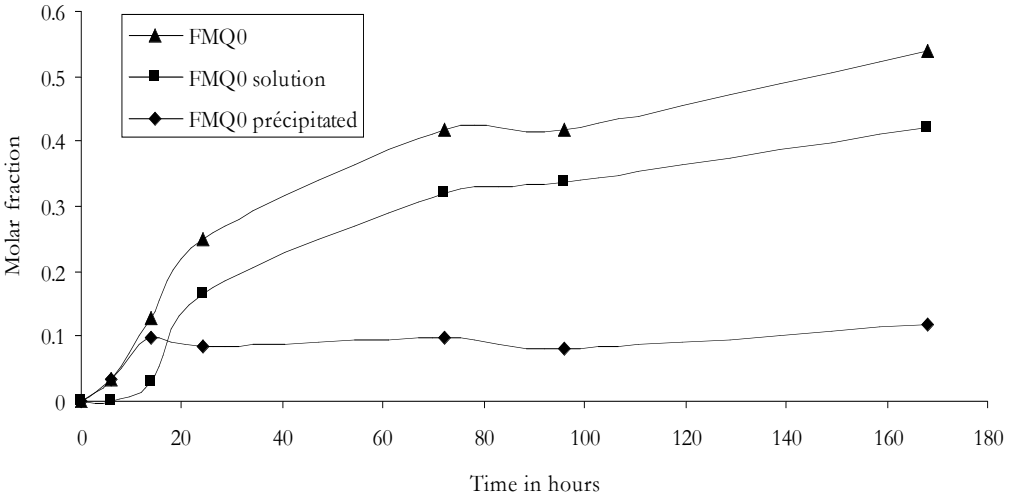

Figure 5: Molar fraction of Q_0 constituted to molar fractions of $Q_{0solution}$ and $Q_{0precipitated}$ according to time for the model reactor with NaOH.

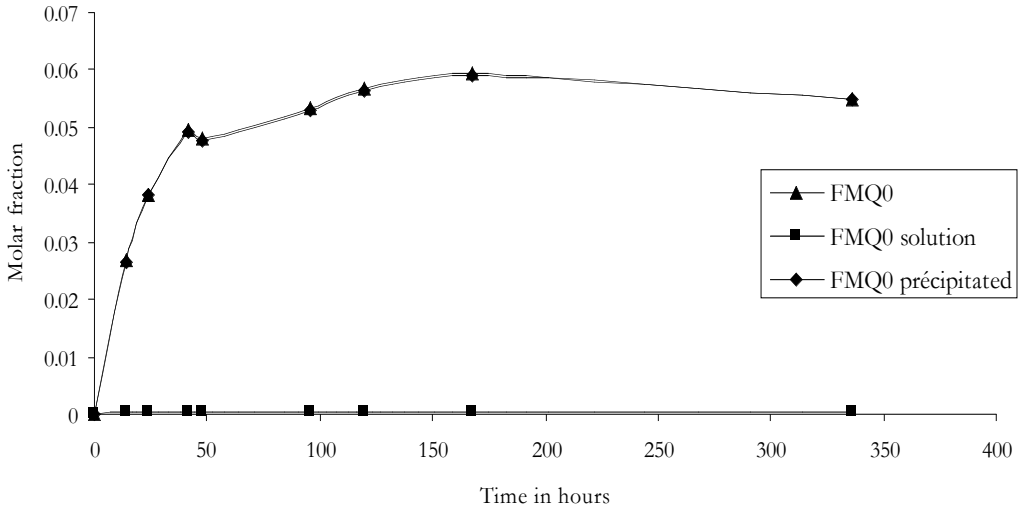

Figure 6: Molar fraction of Q_0 constituted to molar fractions of $Q_{0solution}$ and $Q_{0precipitated}$ according to time for the model reactor with LiOH.

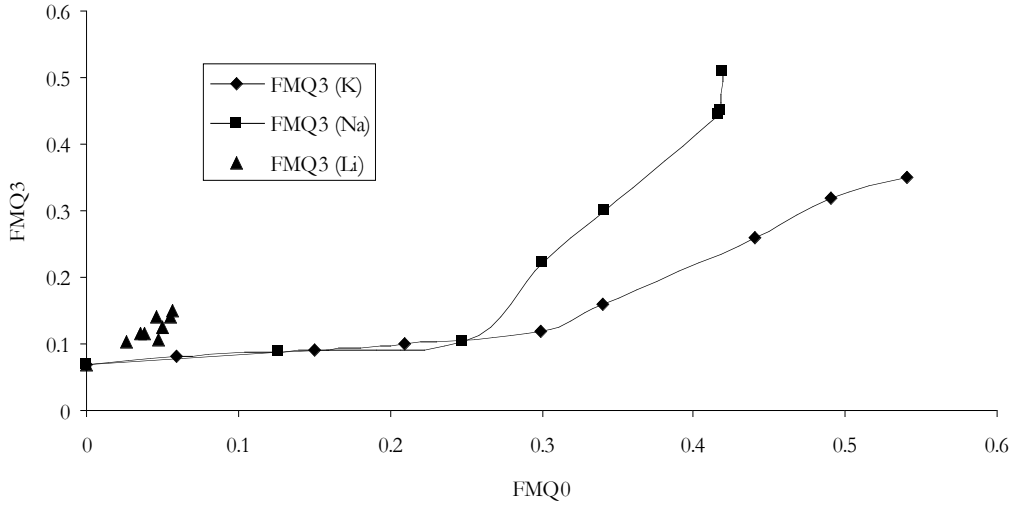

Figure 7: Molar fraction of Q_3 sites according to molar fraction of dissolved silica for 3 model reactors: KOH, NaOH and LiOH.

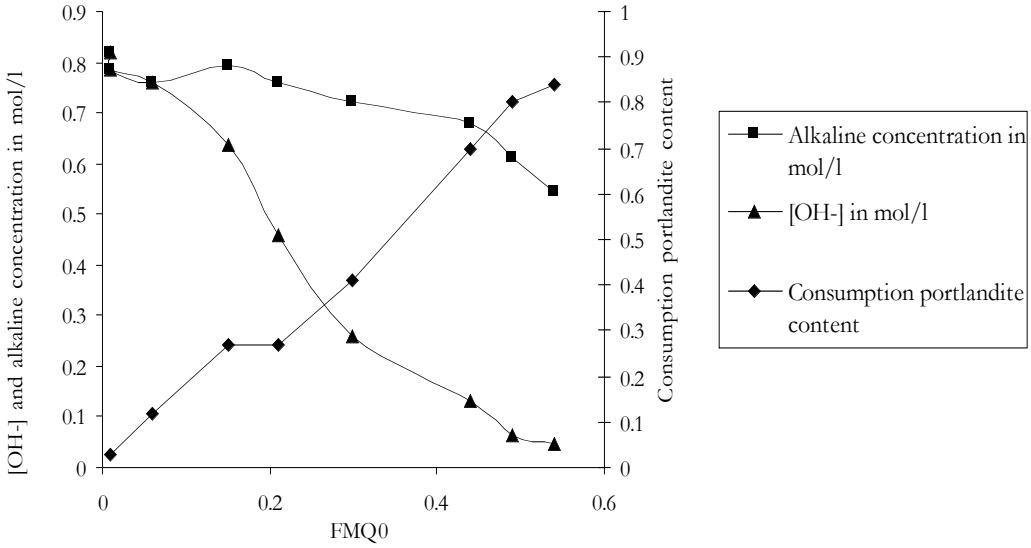

Figure 8: Hydroxyl concentration, alkaline concentration and Consumption portlandite content according to molar fraction of dissolved silica for KOH model reactor.

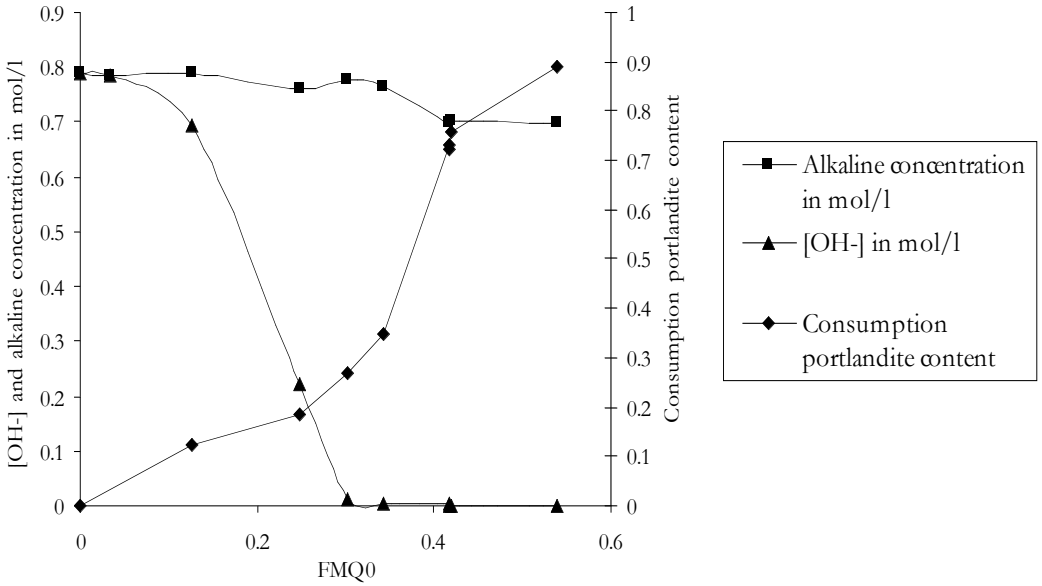

Figure 9: Hydroxyl concentration, alkaline concentration and Consumption portlandite content according to molar fraction of dissolved silica for NaOH model reactor.

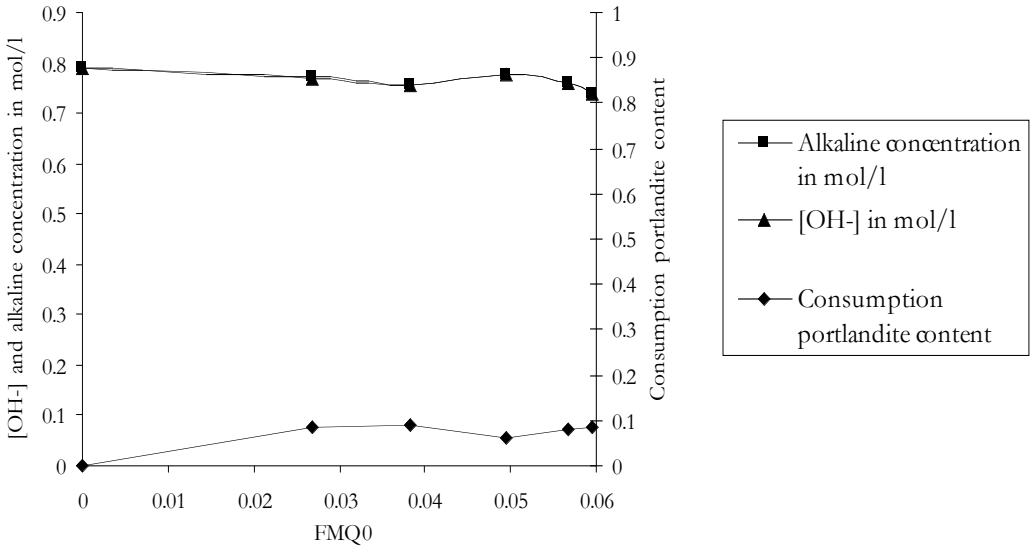

Figure 10: Hydroxyl concentration, alkaline concentration and Consumption portlandite content according to molar fraction of dissolved silica for LiOH model reactor.